

# Solid-state NMR quantum computer with individual access to qubits and some its ensemble developments

K. A. Valiev and A. A. Kokin

Institute of Physics and Technology, Russian Academy of Sciences, Nakhimovskii pr. 36/1, Moscow 117218, Russia, E-mail: qubit@mail.ivvs.ru

## Abstract

Here we made an analysis of the principles of a semiconductor NMR quantum computer and its developments. The known variant of an individual-access computer (B. Kane) and alternative solid-state bulk-ensemble approach versions allowing to avoid some difficulties in implementing the first variant are considered.

## Introduction

Atomic nuclei with a spin quantum number  $I = 1/2$  seem to be the natural candidates for qubits — two-level quantum elements in quantum computers. The early NMR quantum computers approach suggested in 1997 by two teams of researchers independently [1, 2] and then confirmed in experiments [3, 4]. In this approach it was used several diamagnetic organic liquids which individual molecules, having a small number of tied non-equivalent nuclear spins—qubits, acting as almost independent quantum computers. Such an effect is due to the fact that vigorous rotational and translational Brownian motion of molecules in a liquid to a great extent averages both intra- and intermolecular dipole–dipole nuclear spin interactions. Decoherence time of the spin states thus turns out to be relatively large (several seconds or more). Only scalar intramolecular interaction between nuclear spins remains not averaged. It is described by the Hamiltonian  $\sum_{i<j} I_{ij} \hat{\mathbf{I}}_i \hat{\mathbf{I}}_j$  where  $I_{ij}$  is an interaction constant. In particular, for the chloroform molecule  $^{13}\text{C}^1\text{HCl}_3$  this interaction is essential only for proton  $^1\text{H}$  and carbon isotope  $^{13}\text{C}$  and it is this interaction around which unitary quantum operations on qubits have been performed.

Since in liquids the nuclear spins are weakly coupled with the environment, we may restrict our consideration to nuclear spins of an individual molecule (*reduced* quantum ensemble) rather than deal with a huge number of nuclear spins of all molecules of the liquid. For finite temperatures, the reduced ensemble is in the *mixed* state described by a diagonal density matrix. The nonzero elements of this matrix are the *occupancies* of associated spin states. For such a system could perform quantum computation, it should be initialized prior to data entry. *Initialization* means the separation of lower-dimension blocks from the density matrix of the initial mixed state that must have properties similar to those of pure states (a

pure-state diagonal matrix may have only one nonzero element). States described by such matrix are called effective or *pseudo-pure*. All unitary quantum computations are performed using these states. Several approaches to initialization have been reported [1, 2, 4, 5].

In an ensemble computer, many molecules–minicomputers, being nearly independent one another, act in parallel and can thus be controlled by operations on the entire (macroscopic) *volume* of the liquid. These operations are well-known in high-resolution NMR techniques. Access to individual qubits is replaced by simultaneous access to related qubits in all molecules of a bulk ensemble. Computers of this type are called *bulk-ensemble* quantum computers. They, in principle, can operate at room temperature. However, for magnetic fields used in conventional NMR spectrometers (no more than 20 T) relative spin polarization, specifying signals from pseudopure states, is very small even at low temperatures. In addition, the NMR signal intensity exponentially drops with the number of qubits [2]. Therefore, an organic-liquid quantum computer operating at room temperature cannot have much more than 10 qubits in a molecule. Estimates show, however, that a quantum computer of practical value, i.e. with the number of degrees of freedom (or the dimension of the Hilbert space of a set of qubits) larger than in conventional customary computers, must have more than 40 qubits ( $2^{40} \sim 10^{12}$  conventional bits).

Another radically new and still unimplemented design was proposed in [6]. It involves the formation of an artificial multiple-spin system with access to *individual* nuclear spins–qubits. It is suggested to use an semiconductor MOS structure on a  $^{28}\text{Si}$  spinless substrate into a thin layer of which  $^{31}\text{P}$  stable phosphorus isotopes, acting as donors, are implanted. These donors substitute for silicon atoms at the lattice sites, producing shallow impurity states with a large effective Bohr radius, and have a nuclear spin number  $I = 1/2$ . The number of donors or qubits in such artificial "molecules" can be very large.

In this work (see also our article [7]) we analyze in details the principles underlying NMR quantum computer operation (discussed in [6]) and give a some further development. We call attention to the advantages and disadvantages of the early version. Possible alternative ensemble designs of solid-state–based nuclear–spin quantum computers that exploit the same principles but are free of the above disadvantages are next discussed.

## 1 Basic requirements for semiconductor structures

In the discussed Kane’s approach temperatures must be low enough for electrons of the donors occupy only the lower spin state in a magnetic field; i.e.  $T \ll 2\mu_{\text{B}}B/k$  where  $\mu_{\text{B}} = 9.27 \cdot 10^{-24}$  J/T is the Bohr magneton,  $B$  is the induction of an external magnetic field and  $k = 1.38 \cdot 10^{-23}$  J/K is the Boltzmann constant. For  $B \leq 2$  T we have  $T \geq 0.1$  K which is much lower than the temperature for freezing-out donor electron states. Hence, the donors will remain for long in the neutral ground orbital  $S$  state ( $D^0$ –state).

Each donor atom having a nuclear spin must be fairly accurately located under "its" metal gate (gate **A**) separated from the semiconductor by a thin insulator film (for example, several-nanometer-thick silicon oxide). Gates **A** form a linear array of arbitrary length and period  $l$  (one artificial "molecule") (Fig. 1). With the aid of the electric field generated by gates **A** one can affects the electron density distribution near the nuclei in the ground state, thereby *individually* adjusting the resonance frequency of every nuclear spin defined by external

magnetic field and hyperfine nuclear–electron interaction. Thus, quantum operations by selectively applying resonant radio-frequency (RF) pulses to the nuclear spins of particular donors become feasible.

In deciding on the location of the donor atoms under the gate, one should bear in mind that silicon surface is not perfectly smooth; it will always have irregularities like valleys and ridges. Accordingly, the near-surface electric field under the gates at depths on the order of several lattice constants (in silicon, the lattice constant is 0.357 nm) will also be randomly non-uniform. Therefore, the electric field around the donors can be effectively controlled if they are more than 10 nm away from the silicon surface.

The characteristic sizes of the semiconductor structure (Fig. 1) are in a *nanometer* range. Such structures are fabricated with the use of modern nanotechnology techniques, such as epitaxial growth, ultra-high-vacuum (UHV) scanning probe nanolithography based on tunnel or atomic-force microscopes (AFM) [8] and electron-beam or X-ray lithography.

The interaction of the nuclear spins of the donors with the environment can be precluded if the silicon and silicon oxide are enough purified of  $^{29}\text{Si}$  isotope. This isotope has a spin  $I = 1/2$  and is contained in amounts of 4.7% in natural silicon. For the number of silicon atoms per  $\text{cm}^3$  about  $5.0 \cdot 10^{22}$  and the characteristic sizes depicted in Fig. 1, one donor atom occupies a volume of  $20^3 \text{ nm}^3 = 8 \cdot 10^{-18} \text{ cm}^3$ . On the average, less than one  $^{29}\text{Si}$  isotope atom must be present in this volume. Hence, the isotopic purity of silicon should be as high as  $\sim 2 \cdot 10^{-4}\%$ .

In general, III–V semiconductors are inapplicable to quantum computation at this approach, since they do not possess spinless isotopes. However, we assume that spinless semiconductor structures can be built around other Group IV elements. Natural germanium has only one spin isotope  $^{73}\text{Ge}$  ( $I = 9/2$ ) in amounts of 7.76%. Natural carbon has spin isotope  $^{13}\text{C}$  with a spin number  $I = 1/2$  in quantities of 1.1%. Therefore, spinless structures can be made of Ge, Si/Si $_{1-x}$ Ge $_x$ , and SiC materials if they are appropriately purified.

The nuclear spins of  $^{29}\text{Si}$  and  $^{13}\text{C}$  isotope atoms, which produce shallow impurity states in the above structures, can also be viewed as candidates for spins–qubits.

## 2 Electron–nuclear spin system of a donor in a magnetic field

Nuclear and electronic spins of donor atoms in the ground orbital state  $\Psi_0(\mathbf{r})$  interact by hyperfine and dipole–dipole magnetic interactions. After averaging over the orbital electronic state, the latter vanishes, and only *hyperfine* interaction remains, whose Hamiltonian has the form (Fermi formula)

$$\hat{H}_{\text{IS}} = A\hat{\mathbf{I}}\hat{\mathbf{S}}, \quad (1)$$

where

$$A = \frac{8\pi}{3} |\Psi_0(0)|^2 2\mu_{\text{B}} g_{\text{N}} \mu_{\text{N}} \cdot \frac{\mu_0}{4\pi} \quad (2)$$

is hyperfine interaction constant,  $\mu_0 = 4\pi \cdot 10^{-1} \text{ T}^2 \text{ cm}^3 / \text{J}$ ,  $\mu_{\text{N}} = 5.05 \cdot 10^{-27} \text{ J/T}$  is the nuclear magneton, and  $g_{\text{N}} = 2.26$  for  $^{31}\text{P}^1$ . With the experimentally found constant of hyperfine

interaction  $A = 7.76 \cdot 10^{-26}$  J (or  $A/(2\pi\hbar) = 116$  MHz) [9] we obtain for the probability of an electron being on the donor nucleus ( $\mathbf{r} = 0$ )  $|\Psi_0(0)|^2 = 0.43 \cdot 10^{24}$  cm $^{-3}$ .

The electron–nuclear spin Hamiltonian for a donor atom has the form

$$\hat{H} = 2\mu_B \mathbf{B} \hat{\mathbf{S}} - g_N \mu_N \mathbf{B} \hat{\mathbf{I}} + A \hat{\mathbf{I}} \hat{\mathbf{S}}, \quad (3)$$

four energy levels of which are given by the well-known Breit–Rabi formula. For  $I = 1/2$  (the  $z$ -axis is parallel to  $\mathbf{B}$ ) this formula is written as

$$E(F, m_F) = -\frac{A}{4} - g_N \mu_N B m_F \pm \frac{A}{2} \sqrt{1 + 2m_F X + X^2}, \quad (4)$$

where  $X = (2\mu_B + g_N \mu_N)B/A$ ,  $F = I \pm 1/2 = 1, 0$ , and  $m_F = M + m = \pm 1, 0$  if  $F = 1$  or  $m_F = 0$  if  $F = 0$  (Here  $M = \pm 1/2$  and  $m = \pm 1/2$  are  $z$ -projections of electronic and nuclear spins accordingly). The energy levels vs.  $X$  are shown in Fig. 2.

For the energy of the ground spin state,  $F = 0$  and  $m_F = 0$  ( $M = -1/2, m = 1/2$ ); hence, we obtain

$$E(0, 0) = -A/4 - (1/2) \sqrt{(2\mu_B + g_N \mu_N)^2 B^2 + A^2}. \quad (5)$$

For the next, excited energy state,  $F = 1, m_F = -1$ , with the changed nuclear spin state,  $M = -1/2, m = -1/2$ , we have

$$E(1, -1) = A/4 - (2\mu_B - g_N \mu_N)B/2. \quad (6)$$

Thus, the energy difference between the two lower states of the nuclear spin that interacts with an electron whose state remains unchanged is described in simple terms ( $\mu_B \gg \mu_N$  for  $A^2/(2\mu_B B)^2 \ll 1$ ):

$$2\pi\hbar\nu_A = E(1, -1) - E(0, 0) = A/2 + g_N \mu_N B + \frac{A^2}{8\mu_B B} \sim A/2 + g_N \mu_N B. \quad (7)$$

For  $^{31}\text{P}$  donor atoms, the first term in (7) exceeds the second one in fields  $B < 3.5$  T. In this case, the nuclear resonant frequency  $\nu_A$  depends largely on the stationary local magnetic field  $\mathbf{B}_{\text{loc}} = A\mathbf{S}/(g_N \mu_N)$ , which affects the nucleus via electron spin polarization  $\mathbf{S}$ . The external RF field  $b_{\perp}(t)$ , normal to the constant field  $\mathbf{B}$ , in NMR acts on nuclear spin not directly but through the transverse component of electronic polarization  $B_{\text{loc},\perp} \sim AS_{\parallel} b_{\perp}(t)/(g_N \mu_N B)$ . This *gain effect* was first indicated by Valiev in [10].

Now, putting  $B = 2$  T, according to [6], we obtain for the nuclear resonance frequency  $\nu_A = 92.6$  MHz.

### 3 Electronic structure of the ground state of a donor and hyperfine interaction constant

Consider the electronic structure of the ground state of a donor atom. The conduction band in silicon has *six* isoenergetic valleys with minima displaced relative to the Brillouin zone

center by vectors  $\mathbf{k}_j$  ( $j = 1, 2, \dots, 6$ ) ( $|\mathbf{k}_j| = k_0$ ) toward three orthogonal axes of the fourth order. These axes are the axes of symmetry of the crystalline structure of silicon.

Let the direction to neighboring donors ( $x$ -axis) coincide with one of the axes of symmetry of the fourth order, for example [100], i.e., be perpendicular to the directions with whose four of the six energy-valley ellipsoids are aligned. Then, the effective Bohr radius  $a$  of electrons for these *four* symmetric valleys in the indicated direction will be substantially larger than in any other direction, since this radius is defined mainly by the transverse effective mass  $m_t$ , which is much smaller than the longitudinal effective mass  $m_l$ . The value of the effective Bohr radius specifies the extent of the wave function of a donor electron and hence the characteristic scale of the semiconducting structure along  $x$ -axis.

Note that for the same reasons, in germanium, unlike silicon, the direction to a neighbor should be taken along one of six axes of symmetry of the second order, for example, [110]. This axis is perpendicular to four axes of the third order (in the Brillouin zone) along which the valley ellipsoids are aligned.

The orbital wave functions of an electron of a donor atom at the silicon lattice site are written in terms of tetragonal symmetry group representation  $T_d$  and are expressed by superpositions like [11]

$$\Psi(\mathbf{r}) = \sum_{j=1}^6 \alpha_j F_j(\mathbf{r}) \cdot \psi(\mathbf{k}_j, \mathbf{r}), \quad (8)$$

where  $\psi(\mathbf{k}_j, \mathbf{r})$  is a Bloch function quite rapidly varying within a distance comparable to the lattice constant and corresponding to the six  $\mathbf{k}_j$  minima in the Brillouin zone. It is normalized to the unit cell volume  $\Omega$ :

$$\frac{1}{\Omega} \int_{\Omega} |\psi(\mathbf{k}_j, \mathbf{r})|^2 d\mathbf{r} = 1. \quad (9)$$

For silicon, it was found [11] that  $|\psi(\mathbf{k}_j, 0)|^2 = 186 \pm 18$ , so a conduction electron is strongly localized at the lattice site. The wave functions  $F_j(\mathbf{r})$  describe smooth donor-related modulation of the Bloch functions and satisfy the Schrödinger equation with effective masses

$$\left( -\frac{\hbar^2}{2m_l} \frac{\partial^2}{\partial z_j^2} - \frac{\hbar^2}{2m_t} \left( \frac{\partial^2}{\partial x^2} + \frac{\partial^2}{\partial y^2} \right) - \frac{q^2}{4\pi\epsilon_s\epsilon_0 r} - E_d \right) F_j(\mathbf{r}) = 0, \quad (10)$$

where the  $z_j$ -axis is parallel to  $\mathbf{k}_j$  and originates at the donor atom;  $E_d$  are the energy eigenvalues of the donor electron; and  $\epsilon_s = 11.9(\text{Si})$ ,  $\epsilon_0 = 8.85 \cdot 10^{-14} \text{ F/cm}$ .

The ground state of a donor electron in silicon belongs to one-dimensional (non-degenerate) representation  $A_1$  of the tetragonal symmetry group  $T_d$ . The wave function of this state can be represented as the superposition (8) with equal weights  $\alpha_j = \sqrt{1/6}$  [11]:

$$\Psi_0(\mathbf{r}) = \sqrt{1/6} \sum_{j=1}^6 F_j^{(1s)}(\mathbf{r}) \cdot \psi(\mathbf{k}_j, \mathbf{r}). \quad (11)$$

For silicon and germanium, it was performed variational computations with the test modulating wave function [11]

$$F_j^{(1s)}(\mathbf{r}) = (\pi a_t^2 b_l)^{-1/2} \exp[-(\rho^2/a_t^2 + z_j^2/a_l^2)^{1/2}], \quad (12)$$

where  $\rho^2 = x^2 + y^2$ ,  $a_t$  and  $b_t$  are variational parameters for the ground state similar to the 1s state of a hydrogen atom (the ground state under consideration turns into the 1s hydrogen state if  $m_t = m_l$ ). The obtained results somewhat different from the effective Bohr radii with the transverse and longitudinal masses:

$$\begin{aligned} a_t(\text{Si}) &= 2.50 \text{ nm}, & a_l(\text{Si}) &= 1.42 \text{ nm}, \\ a_t(\text{Ge}) &= 6.45 \text{ nm}, & a_l(\text{Ge}) &= 2.27 \text{ nm}. \end{aligned} \quad (13)$$

The results for the ground state energy  $E_{d0}$  were the following (the values in parentheses stand for experimentally found ionization energies  $E_d$ ):

$$\begin{aligned} E_{d0}(\text{Si}) &= -0.029 \text{ eV}(-0.045 \text{ eV}), \\ E_{d0}(\text{Ge}) &= -0.009 \text{ eV}(-0.012 \text{ eV}). \end{aligned} \quad (14)$$

The states of the donor atom with the same function  $F_j^{(1s)}(\mathbf{r})$  but having different weight coefficients for two-dimensional,  $E_1$ , and three-dimensional,  $T_1$ , tetragonal group representations are excited and omitted from consideration.

The theoretically obtained probability of an electron being found in the vicinity of the donor nucleus in silicon,

$$|\Psi_0(0)|^2 = 6(F_j^{(1s)}(0))^2 |\psi(\mathbf{k}_j, 0)|^2 = \frac{6 \cdot 186}{\pi a_t^2 a_l} = 0,042 \cdot 10^{24} \text{ cm}^{-3} \quad (15)$$

is almost 10 times less than the above defined experimental value, and the ionization energy is underestimated by a factor of 1.5. This is explained by the weaker coordinate dependence of the electrical potential in equation (10) produced by a donor atom in silicon at small distances intermediate between the covalent crystallochemical radius of phosphorus, 0.11 nm [12], and the silicon lattice constant, 0.54 nm. In this small region, one can put  $(F_j^{(1s)}(\mathbf{r}))^2 \sim (F_j^{(1s)}(0))^2 \neq (\pi a_t^2 b_l)^{-1}$ . Using the experimental value for  $|\Psi_0(0)|^2$ , we find  $(F_j^{(1s)}(0))^2 = 3.94 \cdot 10^{20} \text{ cm}^{-3}$ .

Consider now a variation of the ground state energy due to a deviation of the potential from the point-charge value [13]:

$$\Delta E_d = \frac{2\pi}{3} (F_j^{(1s)}(0))^2 \frac{q^2}{4\pi\epsilon_s\epsilon_0} \overline{r^2}, \quad (16)$$

where  $\overline{r^2}$  is the average square of the radius of the region where potential deviation takes place. If the deviation of the ground state energy  $\Delta E_d = 0.045 - 0.029 = 0.016 \text{ eV}$ , we find from (16)  $(\overline{r^2})^{1/2} = 0.42 \text{ nm}$ , quite a reasonable value.

It is noteworthy that, while computing  $|\Psi_0(0)|^2$  for germanium with the use of correspondent variational parameters, one should take into account that the centers of isoenergetic ellipsoids are the centers of eight hexagonal Brillouin-zone faces; therefore, the sum over  $j$  will contain only four terms (or four full ellipsoids), and the numerical value of  $|\psi(\mathbf{k}_j, 0)|^2$  will be different. For a  $^{31}\text{P}$  atom, the experimental value of the hyperfine interaction constant is  $A = 15 \cdot 10^{-4} \text{ cm}^{-1} = 45 \text{ MHz}$ , the singlet electronic state factor  $g = 1.56$ , and  $|\Psi_0(0)|^2 = 0,22 \cdot 10^{24} \text{ cm}^{-3}$  [9].

## 4 Hyperfine interaction constant of a donor atom versus electric field

Consider in more details how the external electric field  $E$  induced by the gate potential affects the hyperfine interaction constant  $A$ . We shall assume that the field is aligned with one of the axes of the fourth order. The origin, unlike equation (10), is now on the gate surface rather than at a donor atom (Fig. 1).

With regard to the fact that, at low temperatures, intrinsic semiconductor is essentially a dielectric and also considering that the thickness of substrate  $D \gg l_A \sim c \gg d$  (Fig. 1), we shall express the electric field strength at a donor atom via the potential  $V$  on gate  $\mathbf{A}$ , assuming that the gate is a circular disk of radius  $a = l_A/2$  lying on the surface of a semi-infinite dielectric. The expression for the electrical potential at a point with coordinates  $\mathbf{r} = (\rho, z)$ ,  $\rho^2 = x^2 + y^2$  has the form [14]

$$\varphi(\rho, z) = \frac{2V}{\pi} \arctan \sqrt{\frac{2a^2}{\rho^2 + z^2 - a^2 + [(\rho^2 + z^2 - a^2)^2 + 4a^2z^2]^{1/2}}}, \quad (17)$$

hence, for a line passing through the gate center  $\rho = 0$  near the donor atom, we have

$$\varphi(0, z) = \varphi(0, c) - E_c(z - c) + E'_c(0, c)(z - c)^2/2 + \dots, \quad (18)$$

where

$$\begin{aligned} \varphi(0, c) &= \frac{2V}{\pi} \arctan \frac{a}{c}, \\ E_c = E_c(0, c) &= -\frac{d\varphi(0, c)}{dz} = \frac{2V}{\pi} \frac{a}{a^2 + c^2}, \\ E'_c = E'_c(0, c) &= \frac{dE(0, c)}{dz} = \frac{4V}{\pi} \frac{ac}{(a^2 + c^2)^2} \end{aligned} \quad (19)$$

are the potential, the electric field strength and his gradient at the donor atom. Equation (10) should now be supplemented by the perturbed Hamiltonian  $\hat{H}_\varphi = -q\varphi(0, z)$ .

In the case of the almost homogeneous electric field in the neighborhood of the donor atom (contribution of term with  $E'_c(0, c)$  is small if  $ca_B^*/a^2 \ll 1$ ,  $a_B^* = 8\pi\epsilon_0\epsilon E_{d0}/q^2$  – the effective Bohr radius) a shift in the electronic density distribution relative to the position of the donor atom nucleus causes the same *decrease* in  $A$ , irrespective of the direction of the electric field with respect to  $z$ -axis. A correction to the wave function  $F_j^{(1s)}(c)$  modulating the ground state of a donor (its coordinates are now  $\rho = 0, z = c$ ) is defined by the second-order expression in the perturbation theory. Non-diagonal matrix elements of the perturbation operator between even  $F_j^{(1s)}(\mathbf{r})$  states and odd excited states  $F_j^{(2p)}(\mathbf{r})$  and  $F_j^{(3p)}(\mathbf{r})$ , similar to the  $2p$  and  $3p$  hydrogen states, are not zero. The energies of these excited donor states in silicon [11] are  $E_{2p} = -0.0109$  eV and  $E_{3p} = -0.0057$  eV. Since the excited state functions  $F_j^{(2p)}(c) = F_j^{(3p)}(c) = 0$ , the desired correction, nonzero at  $z = c$ , is given only by that part

of the second-order expression in the perturbation theory proportional to the ground state function  $F_j^{(1s)}(c)$  [13]:

$$\Delta F_j^{(1s)}(V) = -F_j^{(1s)}(c) \frac{q^2 E_c^2}{2} \sum'_m \frac{|\langle 0|(z-c)|m\rangle|^2}{(E_m - E_d)^2}, \quad (20)$$

where  $m = 2p, 3p$ , etc. Since the energy differences between the ground and excited states,  $E_{2p} - E_d = 0.034$  eV,  $E_{3p} - E_d = 0.039$  eV, ..., 0.045 eV, are close to each other, we can estimate this correction through a second-order change in the ground state energy and then through the polarizability  $\chi$  of the atom in an electric field by taking one of the factors in the denominator equal to some mean value  $\delta E \sim 0.04$  eV and carrying it out of the summation sign:

$$\begin{aligned} \Delta F_j^{(1s)}(V) &\sim -F_j^{(1s)}(c) \cdot \frac{q^2 E_c^2}{2\delta E} \sum'_m \frac{|\langle 0|(z-c)|m\rangle|^2}{E_m - E_d} = \\ &= -1/(2\delta E) \cdot (\chi E_c^2/2) \cdot F_j^{(1s)}(c). \end{aligned} \quad (21)$$

The polarizability  $\chi$  of a donor atom in silicon can be estimated by the formula for a hydrogen atom [13] using the effective Bohr radius  $a_B^* = 2$  nm, that leads to  $\chi = 4\pi\epsilon_0 \cdot (9/2)(a_B^*)^3 = 4 \cdot 10^{-32}$  F · cm<sup>2</sup>. Eventually, we have for correction (20)

$$\Delta F_j^{(1s)}(V) = -1.55 \cdot 10^{-12} \cdot E_c^2 \cdot F_j^{(1s)}(c), \quad (22)$$

where electric field  $E_c$  is given in V/cm. From (22), it follows that the relative correction is small when  $E_c \ll 8 \cdot 10^5$  V/cm. For a field-dependent correction to hyperfine interaction constant, one obtains to second-order ( $\sim E_c^2$ ) accuracy

$$\Delta A(V)/A \sim -3.1 \cdot 10^{-12} \cdot E_c^2. \quad (23)$$

Substituting  $E_c = 0.25 \cdot 10^6$  V, found from (19) for  $c \sim 2a \sim 10$  nm, into (23) yields  $\Delta A(V)/A = -0.19V^2$  (here  $V$  in V) or, for a  $V$ -dependent correction to resonance frequency,

$$\Delta\nu_A(V) = \Delta A(V)/A \cdot \nu_A = -17.5 \cdot V^2 \text{ MHz}. \quad (24)$$

This disagrees with results in [6] where a frequency tuning parameter  $\alpha = d\Delta\nu_A(V)/dV \Rightarrow -30$  MHz/V at  $V \Rightarrow 0$  is given. In general, the linear part of the  $\Delta\nu_A$  vs.  $V$  dependence may be attributed to different causes. One of this is a non-homogeneity of the electric field (if  $ca_B^*/a^2 \sim 1$ ), and other is the built-in electric field in the semiconductor. In the first case it is necessary to take into account the last member of the expression (18) which have the first-order perturbation theory nonzero value. The second case can take place when the work functions of the gate and substrate, which determine flat-band voltage  $V_{FB}$ , are distinguish. In this case, one should put  $V^2 \Rightarrow (V_{FB} + V)^2$  in the above expressions. If for example, we put  $V_{FB} \sim 0.6$  V,

$$\begin{aligned} \Delta\nu_A(V) &\sim -17.5 \cdot (V_{FB} + V)^2 = \\ &= -6.3 - 21.0 \cdot V - 17.5 \cdot V^2 \text{ MHz}. \end{aligned} \quad (25)$$

Note, that, as  $V$  and  $V_{\text{FB}}$  approach 1 V, the second-order expressions of the perturbation theory become poor approximation and corrections with  $E_c^3$  must be included in (22).

The relative error in the hyperfine interaction constant  $\overline{\delta A}/A$  due to technological inaccuracy  $(\overline{\delta\rho})^2$  in placing donor atoms in the  $z$ -axis is defined from (17) and (23) by the ratio  $\sim 2\overline{\delta\rho}^2/a^2$  for  $c/a \ll 1$  and  $\sim 2\overline{\delta\rho}^2/c^2$  for  $c \sim a$ . The condition  $\overline{\delta A}/A \ll 1$  then specifies the *lower limit* for the parameters  $c$  and  $a \sim l_A/2$ .

## 5 Electron–nuclear spin system for two interacting donor atoms

The distance  $l$  between donors, as well as the period of the semiconductor structure, is taken small enough. In this case, the constant  $J$  of effective exchange electron–electron interaction  $J(\hat{\mathbf{S}}_a\hat{\mathbf{S}}_b)$  between two hydrogen-like neighbors a and b due to partial overlap of their electronic wave functions in the corresponding direction is the most sensitive to the field of the gate  $\mathbf{J}$ .

The total spin Hamiltonian for such a "molecule" is

$$\hat{H} = 2\mu_B\mathbf{B}(\hat{\mathbf{S}}_a + \hat{\mathbf{S}}_b) + J\hat{\mathbf{S}}_a\hat{\mathbf{S}}_b + \Delta\hat{H} = \hat{H}_0 + \Delta\hat{H}, \quad (26)$$

where

$$\Delta\hat{H} = \hat{H}_a + \hat{H}_b = -g_N\mu_N B(\hat{I}_{za} + \hat{I}_{zb}) + A_a\hat{\mathbf{I}}_a\hat{\mathbf{S}}_a + A_b\hat{\mathbf{I}}_b\hat{\mathbf{S}}_b. \quad (27)$$

In the absence of external magnetic field, for a positive value of the exchange interaction constant  $J > 0$ <sup>2)</sup> ground state  $^1\Sigma$  of the "molecule" is singlet. In [6], for well-separated hydrogen-like atoms, an asymptotic expression that does not include oscillations due to interference of the Bloch functions for various valleys was employed. In terms of the designations adopted in our work, it has the form [15]<sup>3)</sup>

$$J(l) \approx 1,6 \cdot \frac{q^2}{4\pi\epsilon\epsilon_0 a_t} \cdot (l/a_t)^{5/2} \exp(-2l/a_t), \quad (28)$$

where  $a_t = 3$  nm for silicon (in [6], this variational parameter was used slightly lower:  $a_t = 2.5$  nm).

According to variational parameters (13), the extent of the wave function of a donor-atom electron, which is specified by  $a_t$ , in germanium turns out to be 2.6 times greater than in silicon. Accordingly, the distance at which the desired overlap of the wave functions of neighboring donors is achieved also increases. Thus, in the case of germanium, the scale of the semiconductor structure can be *considerably extended* if the axes of symmetry are properly oriented.

We shall omit for a while the interaction with nuclear spins in (26), which here is a small perturbation, and after diagonalization of the Hamiltonian we arrive at three triplet

---

<sup>3)</sup> This asymptotic expression differs from the known Sugiura's Heitler–London approximation, which gives a physically impossible positive value at extremely large  $l/a_t > 49,5$ .

( $S = 1, M = 0, \pm 1$ ) and one singlet ( $S = 0, M = 0$ ) energy levels for a dual-spin system ( $M = M_a + M_b$  - the projection of total electronic spin)

$$E_0(S, M) = J[S(S + 1)/2 - 3/4] + 2\mu_B BM. \quad (29)$$

Varying the potential of gates  $\mathbf{J}$ , located between gates  $\mathbf{A}$ , one can control the electronic density between neighboring donor atoms and thus the overlap of the wave functions of electrons localized on neighboring donors a and b, as well as the constant of their exchange interaction  $J$  and the constant of indirect scalar interaction between their nuclear spins  $I_{ab}$ .

From Fig. 3, it follows that, for  $J = 2\mu_B B$ , the singlet and one triplet levels are crossed as  $B$  grows. In this range of the parameter  $J$ , even rather weak effects may essentially change the structure of the ground electronic state of the "molecule". The relationship  $J(l) = 2\mu_B B$  defines the necessary interdonor distance, which was estimated in [6]. For  $B = 2$  T, it is  $l \sim 10 - 20$  nm  $\gg a_t$ ; hence, the *upper limit* for the size of gates  $\mathbf{A}$  in such fields is  $l_A \sim 10$  nm. If germanium is used instead of silicon, rough estimates using the above values of the variational parameters yield much greater sizes:  $l \sim 25 - 50$  nm and  $l_A \sim 25$  nm.

Consider now hyperfine splitting of "molecular" levels due to the Hamiltonian of perturbation  $\Delta\hat{H}$  (27) ( $J \gg A_a, A_b$ ). The main interest is the splitting of electronic levels, crossing and especially an anticrossing of states near the level crossing point.

We shall take into account, following on [16], that commutator  $[\hat{S}_{za} + \hat{S}_{zb} + \hat{I}_{za} + \hat{I}_{zb}, \hat{H}] = 0$ . Since the total electron-nuclear spin projection in the magnetic field direction  $m_a + m_b + M_a + M_b = m + M$  is conserved, matrix  $16 \times 16$  that represents the total Hamiltonian, falls into five reduced matrices, corresponding to values  $m + M = 0, \pm 1, \pm 2$ . The four states, some of which are used for measurements of the nuclear spin states, correspond to  $m + M = -1$ .

We shall represent the perturbation Hamiltonian (27) as the sum of the secular and nonsecular parts:  $\Delta\hat{H} = \Delta\hat{H}_{\text{sec}} + \Delta\hat{H}_{\text{nsec}}$ , where

$$\Delta\hat{H}_{\text{sec}} = -g_N\mu_N B(\hat{I}_{za} + \hat{I}_{zb}) + (1/2)(A_a\hat{I}_{az} + A_b\hat{I}_{bz})(\hat{S}_{az} + \hat{S}_{bz}), \quad (30)$$

$$[\Delta\hat{H}_{\text{sec}}, \hat{H}_0] = 0. \quad (31)$$

The paired nuclear spins  $I_{a,b} = 1/2$  of the atoms a and b may be in three triplet ( $I = I_a + I_b = 1, m = m_a + m_b = 0, \pm 1$ ) and one singlet ( $I = I_a - I_b = 0, m = 0$ ) states.

States of the electronic-nuclear spin system will be designated as  $|S, M; I, m\rangle$ . They are eigenstates of the total Hamiltonian if the nonsecular part of hyperfine interaction  $\Delta\hat{H}_{\text{nsec}}$  is neglected.

Let us concentrate here on two cases:

1) For  $J < 2\mu_B B$ , the lowest triplet state ( $S = 1, M = -1$ ) is the ground electronic state (Fig. 3). First-order energy corrections to (29) within the perturbation theory depend on diagonal matrix elements of  $\Delta\hat{H}$ :

$$\Delta E_1(S, M; I, m) = \langle S, M; I, m | \Delta\hat{H} | S, M; I, m \rangle \quad (32)$$

In this approximation, from the ground electronic level  $E_0(1, -1)$  only three sublevels determined by the secular part of Hamiltonian are split:

$$\begin{aligned} \Delta E_1(1, -1; 1, -1) &= g_N\mu_N B + (A_a + A_b)/4, \\ \Delta E_1(1, -1; 0, 0) &= \Delta E_1(1, -1; 1, 0) = 0, \\ \Delta E_1(1, -1; 1, 1) &= -g_N\mu_N B - (A_a + A_b)/4, \end{aligned} \quad (33)$$

The states  $|1, -1; 1, 0\rangle$  and  $|1, -1; 0, 0\rangle$  that have the same value  $m + M = -1$ , remain degenerated. In the next approximation determined by the nonsecular part of hyperfine interaction, the lowest level  $E_0(1, -1)$  in the electronic triplet for  $J < 2\mu_B B$  is split into four sublevels.

2) For  $J > 2\mu_B B$ , the electronic singlet  $|0, 0\rangle$  is the ground electronic state. In the first approximation, the singlet ground electronic level is split into next three hyperfine sublevels<sup>4)</sup>:

$$\begin{aligned}\Delta E_1(0, 0; 1, -1) &= g_N \mu_N B, \\ \Delta E_1(0, 0; 0, 0) &= \Delta E_1(0, 0; 1, 0) = 0, \\ \Delta E_1(0, 0; 1, 1) &= -g_N \mu_N B,\end{aligned}\tag{34}$$

Among them one state  $|0, 0; 1, -1\rangle$  have  $M + m = -1$ . If nonsecular part of hyperfine interaction is accounted this state participates in an anticrossing process for the state  $|1, -1; 0, 0\rangle$ .

Near the crossing point  $C$  for the ground electronic states the nonsecular part of hyperfine interaction  $\Delta \hat{H}_{\text{nsec}}$  has next four nonzero non-diagonal matrix elements between states with the same values  $m + M$ :

$$\begin{aligned}\langle 0, 0; 0, 0 | \Delta \hat{H}_{\text{nsec}} | 1, -1; 1, 1 \rangle &= -(A_a + A_b)/4, \\ \langle 0, 0; 1, -1 | \Delta \hat{H}_{\text{nsec}} | 1, -1; 1, 0 \rangle &= (A_a - A_b)/4, \\ \langle 0, 0; 1, -1 | \Delta \hat{H}_{\text{nsec}} | 1, -1; 0, 0 \rangle &= (A_a + A_b)/4, \\ \langle 0, 0; 1, 0 | \Delta \hat{H}_{\text{nsec}} | 1, -1; 1, 1 \rangle &= (A_a - A_b)/4.\end{aligned}\tag{35}$$

They describe the splitting of the hyperfine states that intersect in the absent of  $\Delta \hat{H}_{\text{nsec}}$ . In order to find out the picture of the anticrossing process we shall choose then as basis the next four states of the electron–nuclear spin system with  $M + m = -1$ :  $|S, M; I, m\rangle = |1, -1; 0, 0\rangle, |1, -1; 1, 0\rangle, |1, 0; 1, -1\rangle$  and  $|0, 0; 1, -1\rangle$ . The reduced Hamiltonian can be represented then by matrix

$$\hat{H}_0 = \begin{pmatrix} J/4 - 2\mu_B B & (A_a - A_b)/4 & -(A_a - A_b)/4 & (A_a + A_b)/4 \\ (A_a - A_b)/4 & J/4 - 2\mu_B B & (A_a + A_b)/4 & -(A_a - A_b)/4 \\ -(A_a - A_b)/4 & (A_a + A_b)/4 & g_N \mu_N B + J/4 & -(A_a - A_b)/4 \\ (A_a + A_b)/4 & (A_a - A_b)/4 & -(A_a - A_b)/4 & g_N \mu_N B - 3J/4 \end{pmatrix}\tag{36}$$

If for simplicity to assume here  $A_a = A_b = A$ , the matrix eigenvalues can be expressed by the simple equation:

$$\begin{aligned}[(J/4 - 2\mu_B B - E) \cdot (g_N \mu_N B - J/4 - E) - A^2/4]^2 - \\ - [(J/4 - 2\mu_B B - E) \cdot J/2]^2 = 0.\end{aligned}\tag{37}$$

In this case Hamiltonian is symmetric, as in the absence of hyperfine interaction, with respect to interchanging donors a and b and eigenstates of Hamiltonian are divided into two

---

<sup>4)</sup> In [7] we have made mistakes for the values  $\Delta E_1(0, 0; 0, 0)$  and  $\Delta E_1(0, 0; 1, 0)$ .

symmetric ( $I, S = 1$ ) and two antisymmetric ( $I + S = 1$ ) states, that are correspondent to the superpositions of the paired states  $|1, -1; 1, 0\rangle, |1, 0; 1, -1\rangle$  and  $|1, -1; 0, 0\rangle, |0, 0; 1, -1\rangle$  with eigenvalues [16]:

$$\begin{aligned} E_{\pm}^s &= g_N \mu_N B/2 + J/4 - \mu_B B \pm \sqrt{(\mu_B B + g_N \mu_N B/2)^2 + (A/2)^2}, \\ E_{\pm}^a &= g_N \mu_N B/2 - J/4 - \mu_B B \pm \sqrt{(\mu_B B + g_N \mu_N B/2 - J/2)^2 + (A/2)^2}. \end{aligned} \quad (38)$$

The splitting of the states  $|1, -1; 1, 0\rangle$  and  $|1, -1; 0, 0\rangle$  degenerated in the first approximation is now

$$\begin{aligned} E_-^s - E_-^a &= 2\pi\hbar\nu_J \sim \frac{(A/2)^2}{2\mu_B B - J} - \frac{(A/2)^2}{2\mu_B B}, \quad \text{for } J \ll 2\mu_B B, \\ E_-^s - E_-^a &= 2\pi\hbar\nu_J \sim A/2, \quad \text{for } J = 2\mu_B B. \end{aligned} \quad (39)$$

The energy  $2\pi\hbar\nu_J$  is the energy of transition of paired nuclear spins from the upper triplet state to the singlet state. It is known that such splitting can be described by spin Hamiltonian like  $I_{ab}\hat{\mathbf{I}}_a\hat{\mathbf{I}}_b$ , where  $I_{ab} = 2\pi\hbar\nu_J$  is the indirect "exchange" integral for nuclear spins. For  $B = 2$  T and  $J/2\pi\hbar = 30$  GHz  $< 2\mu_B B/2\pi\hbar = 57$  GHz,  $\nu_J$  was estimated at  $\nu_J = 75$  kHz  $\ll \nu_A = 92.6$  MHz [6]. Note that the frequency  $\nu_J$  grows as we approach the crossing point of the unperturbed levels  $E_0(1, -1)$  and  $E_0(0, 0)$  and vanishes at  $J \Rightarrow 0$ .

As it follows from (38), the electron-nuclear antisymmetric state  $|1, -1; 0, 0\rangle$  for  $J < 2\mu_B B$  undergoes the transformation into anticrossed antisymmetric state  $|0, 0; 1, -1\rangle$  for  $J > 2\mu_B B$ . That is, the electron and nuclear subsystems exchange their states with the *opposite transfer of nuclear spin states* near the crossing point. The electron-nuclear symmetric state  $|1, -1; 1, 0\rangle$  for  $J < 2\mu_B B$  does not anticross with any ground electronic states  $|0, 0\rangle$  for  $J > 2\mu_B B$  and does not change nuclear spin states. Note that the splitting of symmetric and antisymmetric states levels for  $J \gg 2\mu_B B$

$$E_-^s - E_-^a = 2\pi\hbar\nu_J \sim J - 2\mu_B B \quad (40)$$

is more then (39) for  $J \ll 2\mu_B B$ . Under these conditions, the constant of indirect scalar interaction  $I_{ab}$  between the nuclear spins of the donor atoms a and b also radically changes.

The hyperfine splitting of triplet and singlet electronic levels near the point  $C$  is shown schematically in Fig. 3.

## 6 Measurement of nuclear spin states

Measurement of individual nuclear spin states is one of the important problems. We will discuss here this very briefly.

The nuclear spin state is set for  $J \ll 2\mu_B B$ , where nuclear spins are handled with NMR methods by applying RF pulses of resonance frequency. It is suggested to measure this state in two stages [6]. Suppose that after quantum computation at  $J \ll 2\mu_B B$  two electrons, both on its donor atom, are initially in the triplet state that is in the  $|1, -1\rangle$  state, the whole electron-nuclear system is either in  $|1, -1; 1, 0\rangle$  or in  $|1, -1; 0, 0\rangle$  state. By *adiabatically*

increasing of the exchange parameter to  $J > 2\mu_B B$  in a process of the crossing point passage we lead to the electron-nuclear system transition from one antisymmetric state  $|1, -1; 0, 0\rangle$  to other  $|0, 0; 1, -1\rangle$  at the same total spin projection and allow *transfer the information* from nuclear to the electron spin subsystem.

In addition, if the energy of bound for an electron at one neutral donor (it is usually small) is more then its energy of attraction to the neighboring ionized donor ( $D^+$ –state), the electron will be found near the neutral donor ( $D^-$ –state or helium-like atom) and charge transfer from one donor to the other will occur. This may be reach also by the corresponding change of the gate **A** electric potential. Therefore, *a charge transfer* from one donor to another takes place. It is supposed [6] that this process can be detected with highly sensitive *single-electron capacitive techniques*.

It is important to note that the electrical measurements time should be significant less then the time of electron spin–lattice relaxation, that at low temperatures exceeds  $10^3$  s. In the case of an electrical control and electrical measurements the states of qubits the noise in electrical circuits are also significant. They cause fluctuations of the nuclear resonant frequencies  $\nu_A$  and  $\nu_J$  and lead in result to decoherence and dissipation of quantum states and to quantum errors in the process of calculations.

The detailed theoretical investigation of the electrical single-spin measurement method of electron and nuclear spin states by using single-electron transistors in simpler semiconductor structures with one double donor (in particular Te) was given in [17]. Another scheme for measurement of the state of single spin based on the single-electron turnstile and injection of spin polarized electrons from magnetic metal contacts is proposed in [19].

## 7 Bulk-ensemble solid-state quantum NMR computers

The approach suggested in [6] can solve a number of problems typical for the considered individual-access computing. First, to initialize the starting state of the system, it will suffice to go to low temperatures  $T \ll 2\mu_B B/k$ , at which each electronic spin of a donor atom is in the pure quantum ground state and thermal fluctuations are suppressed. Accordingly, the nuclear spins are also in the pure state. No special procedure to separate pseudopure states is required in this case. Second, the number of spins–qubits in this case is unlimited, which opens the door to creating an actual many-qubit quantum computer instead of demonstrating only quantum principles with the simplest spin systems on organic molecules. Third, there appears a possibility to detect, with single-electron techniques, electron transfer between adjacent **A** gates and thus to sense the state of individual nuclear spins. In [6], the possibility of creating hybrid quantum–classical systems was also noted. Here, quantum nuclear-spin devices are supplemented with conventional integrated circuits when many-qubit systems are difficult to obtain.

However, there are certain difficulties in implementing a quantum computer on individual donor atoms that was suggested in [6]. These are, first of all, small signal from the spin of an individual atom, the need for use of high sensitive single-electron measurements, then the need for precision regular donor arrangement with nanometer scale that matches the gate chain, and at last the need for use of low temperatures.

As an alternative, we will briefly discuss here another feasibility of a bulk-ensemble silicon quantum computer. In this case, unlike the structure suggested in [6], gates **A** and **J** form a chain of narrow ( $l_A \sim 10$  nm) and long (several micrometers) strips along which donor atoms  $L$  distant from each other are placed (Fig. 4). Thus, they form a quasi-one-dimensional regular structure. It can be considered also a random distribution of donors under gates.

We shall consider here only *two cases*.

Let  $L$  be so much larger than  $l$  that exchange spin interaction between electrons of donor atoms along the strip gates ( $y$ -axis) is negligibly small; i.e.,  $J(L), kT \ll J(l), 2\mu_B B$ . Then, such a system breaks down into independent chains of the donor atoms in the direction transverse to the gates ( $x$ -axis). In that case, the regularity of donor structure along the strip gates does not play any role. The gates form an ensemble of independent equivalent multiple-qubit computers—artificial "molecules" whose electronic spins are initially aligned with the field. Accordingly, all nuclear spins—qubits are also similarly oriented. An output signal in this system, as in liquids, will be proportional to the number of the "molecules" or donor atoms under a strip gate **A**. For example, for number of "molecules" more than thousand the length of the strips should be more than ten micron.

One would expect that with the bulk-ensemble approach, where many "molecules" work simultaneously, electrical measurements would be greatly simplified.

A more complicated situation appears when  $L < l$ . In this case,  $J(L) \gg 2\mu_B B, J(l) \gg kT$ , and exchange interaction between localized electronic spins along the strip gates will be favorable for producing one-dimensional antiferromagnetically ordered chains, that may be considered at low temperatures as a pure macroscopic quantum state. The neighboring electronic spins in the antiferromagnetic chain in the absence of the field are oppositely oriented. Due to hyperfine interaction in the ground state, nuclear spins will also be oriented according to the electronic spin direction in the resultant field and will form in chains an antiferromagnetic type order.

The nuclear resonant frequencies  $\nu_A$  of neighboring nuclear spins will be different for each of the magnetic one-dimensional subarrays in the chain:  $2\pi\hbar\nu_A^\pm \sim |g_N\mu_N B \pm \frac{A}{2}|$ . As in the case of electronic spins oriented only in the external field, the RF field has a greater effect on a nuclear spin because of hyperfine interaction. A resulting NMR signal tuned only to one of the frequencies  $\nu_A^\pm$  will be proportional to half the number of nuclear spins in the antiferromagnetic chain or half the number of donor atoms under the gate **A**.

The selective RF  $\pi$ -impulse tuned to one of the resonant frequency can invert the nuclear spins state of one subarray in a chain and the nuclear spins of whole chain will acquire quasi-one dimensional ferromagnetic ordering while the neighboring chain will remain in the antiferromagnetic state.

Let now the electronic spins of the such two neighboring chains are also setting for  $J(l) \ll 2\mu_B B$ , that is let they and half the number of nuclear spins in the chains are in the state with the same orientations (triplet states of the spin pairs), while other half the number of nuclear spins is in the state with opposite orientations (singlet states of spin pairs). By adiabatically increasing of the exchange parameter by means of **J**-gate potential varying to  $J(l) > 2\mu_B B$  in the passage of the crossing point we lead for each electron-nuclear pair of two neighboring chains to the transition from one antisymmetric state into other antisymmetric state. The triplet electronic pairs ground state of two neighbor chains must pass to the singlet

state. The subarray of nuclear spins which is in the state with opposite orientation of nuclear spins relative to the subarray of neighboring chain will transit in the state with the same orientations. The electron subsystem of two chains simultaneously passes in antiphase state and at the same time to the half period shift of antiferromagnetically ordered electronic spins in the one chain relative to the other. The nuclear subsystem of the both chains becomes ferromagnetically ordered. Again, the Pauli principle allows two electrons to be now on the one site, if it is energetically profitable, that it allows transfer electrons between the neighboring chains and destruction the antiferromagnetic ordering in the chains. This process can be detected more easy than by means of highly sensitive single-electron spin states detecting methods.

The relaxation time  $T_2$  of nuclear spins, which characterizes the *decoherence* time of their quantum states, depends largely on fluctuations of local fields that are determined mainly by interactions between nuclear and electronic spins of different atoms. If the times of electronic spin–spin and spin–lattice relaxations in a semiconductor ( $\tau_2$  and  $\tau_1$ , respectively) are short, that play the correlation times of fluctuating fields, electron–nuclear dipole–dipole and scalar interactions will be strongly averaged, like in liquids, and the time  $T_2$  will be large. Only the scalar part of indirect interaction between the nuclear spins of donors  $I_{ab}\hat{\mathbf{I}}_a\hat{\mathbf{I}}_b$  will remain non-averaged.

However, when the states of individual nuclear spins are determined by electrical techniques, the time  $\tau_1$  of electronic spin–lattice relaxation must be sufficiently large (several thousands of seconds) for the state of electronic spin have no time to relax during the electric measurements. This again indicates the need for low temperatures [6, 16]. In that case, for large enough distance between donors, large times  $T_1$  and  $T_2$  are provided mainly by the *small amplitudes* of fluctuating local hyperfine fields. In insulators at low temperatures this fields are determined by electron-phonon mechanism. In particular it was demonstrated [18] that the phonon induced spin-lattice nuclear relaxation time  $T_1$  for low temperatures in silicon is very large. In the case of antiferromagnetically ordering at low temperatures the fluctuating local fields are determined also by the interaction of nuclear spin with electron spin waves [21].

The decoherence is associated also with *noise voltages* across the gates **A**. To suppress the decoherence of different origin ideas similar to those underlying high-resolution NMR methods may be used [20].

Upon forming structures with closely spaced and narrow gates **A**, it would be more appropriate the lower arrangement of strip gates **J**. In this case, gates **A** can be made wider for the same interdonor distance along the  $x$ -axis. If we completely do away with electrical measurements of individual states, the control gates **J** become unneeded and the semiconductor structure simpler. Scalar interaction between nuclear spins of donor atoms through their electronic states, as well as their resonant frequency, will be controlled only by gates **A** and external magnetic field.

An another interesting approach to implementation of a solid state *ensemble* quantum computer was described in [22], where it was considered a lattice of nuclear spins  $1/2$  having periodic structure of ABCABCABC... type in two or three dimensions, where A,B,C—are nuclear spins only of *three types* with different resonance frequencies. It is supposed that the nuclei at three sites are embedded in a crystal lattice of some solid state compound with

non-spinning nuclei and initialized with all spins at the ground  $|0\rangle$  state. Each ABC-units of this superlattice can be used to store quantum information by setting one of spin up or down. This information can be moved around via some quantum cellular shifting mechanism. Cascading *unitary quantum SWAP* operations of  $A \leftrightarrow B$ ,  $B \leftrightarrow C$ ,  $C \leftrightarrow A$ ,  $A \leftrightarrow B$ ,  $\dots$ , every which is achieved by cascading three quantum controlled NOT gates, can be used for this process. An ancillary donor nucleus D with spin 1/2 in the proximity of an A-site can serve as the input/output port.

*Universal* quantum logic is implemented with the aid of two-body interactions between two spins at D and a nearby site. A local environment region, about tens of ABC-units along all three dimensions provides a large quantum system with *a number of qubits over thousands* and only three types of nuclear spins. The whole crystal contains a *huge ensemble* of such identical NMR quantum computers—large artificial "molecules". The information in this case can be input by setting the D-spins to desired states then transferring to the nearest A-spins via the quantum SWAP operation. All these can be done selectively if the specified quantum transitions are driven by RF fields with distinguished frequencies. After this, the D-spins are reset to the  $|0\rangle$  state.

The state of any qubits can be measured by moving it to the A-site nearest to the D-spins, then by swapping  $A \Rightarrow D$ . Finally the state of the D-spins is measured by using NMR techniques. The proposed NMR quantum computer by the authors opinion can be easily scaled up and may work at low temperature to overcome the problem of exponential decay in signal-to-noise ratio. However, authors of the article [22] did not made any numerical estimations and discuss any possibility of a concrete realization of this idea.

In conclusion, we will consider briefly possible nonelectric approaches that would allow ensemble solid state computers to actually operate at room temperature. Several such approaches are available from the literature.

Highly sensitive optical measurements of a change in Overhauser shift in exciton optical spectra were discussed in [23]. The shift changed as a result of nuclear polarization in GaAs/Al<sub>x</sub>Ga<sub>1-x</sub>As quantum dots. In-plane spatial resolution of  $\sim 10$  nm and a sensitivity of  $10^4$  nuclear spins at 6 K were achieved. This ensemble variant, based on optical detection, requires considerable redesign of the structure for laser radiation can strike required regions. Note that the sensitivity attained in [23] is sufficient just for the ensemble approach. However, there are not well-known sensitive optical measurements for semiconductor structures in which silicon, germanium etc. are used.

At higher temperatures, a number of spins will pass into the excited state, while others will remain in the ground state. Of the latter spins, one can construct the pseudopure state, using methods mentioned in the Introduction for the ensemble approach. Another way to keep as many nuclear spins as possible in the ground state is to orient them not only with a permanent external magnetic field but also with dynamic methods, such as optical pumping [24], which make possible the orientation of nuclear spins as high as nearly 100% even at room temperature. However, this can be done only for direct-gap semiconductors like III–V compounds. In the case of silicon or germanium this property of the band structure may be received, if the single crystals will be properly strained.

The authors are grateful to V.A.Kokin and L.E.Fedichkin for critical reading of the article and for useful remarks.

## References

- [1] Gershenfeld, N.A., and Chuang, I.L., Bulk Spin-Resonance Quantum Computation, *Science*, 1997, vol. 275, pp. 350–356.
- [2] Chuang, I.L., Gershenfeld, N., Kubinec, M.G., and Leung, D.W., Bulk Quantum Computation with Nuclear Magnetic Resonance: Theory and Experiment, *Proc. Roy. Soc. London*, 1998, vol. A454, no. 1969, pp. 447–467.
- [3] Cory, D.G., Price, M.D., and Havel, T.F., Nuclear Magnetic Resonance Spectroscopy: An Experimentally Accessible Paradigm for Quantum Computing, *Physica D*, 1997, vol. 120, no. 1–2, pp. 82–101.
- [4] Cory, D.G., Fahmy, A.F., and Havel, T.F., Ensemble Quantum Computing by NMR Spectroscopy, *Proc. Nat. Acad. Sci. USA*, 1997, vol. 94, no. 5, pp. 1634–1639.
- [5] Knill, E., Chuang, I., and Laflamme, R., Effective Pure States for Bulk Quantum Computation, *Phys. Rev. A: Gen. Phys.*, 1998, vol. 57, no. 5, pp. 3348–3363.
- [6] Kane, B.E., A Silicon-Based Nuclear Spin Quantum Computer, *Nature (London)*, 1998, vol. 393, pp. 133–137.
- [7] Valiev, K.A. and Kokin, A.A., Semiconductor NMR Quantum Computers with Individual and Ensemble Access to Qubits, *Microelektronika*, 1999, vol. 28, no. 5, pp. 326–337 (in Russian).
- [8] Lyding, J.W., UHV STM Nanofabrication: Progress, Technology Spin-Offs, and Challenges, *Proc. IEEE*, 1997, vol. 85, no. 4, pp. 589–600.
- [9] Ludwig, G., and Woodbury, H., *Electron Spin Resonance in Semiconductors*, New York: Academic Press, 1962.
- [10] Valiev, K.A., Magnetic Resonance on Nuclei of Paramagnetic Atoms, *Zh. Eksp. Teor. Fiz.*, 1957, vol. 33, no. 4(10), pp. 1045–1047 (in Russian).
- [11] Kohn, W., Shallow Impurity States in Silicon and Germanium, *Solid State Physics*, Seitz, F. and Turnbull, D., Eds., New York: Academic Press, 1957, vol. 5, pp. 257–320.
- [12] Kittel, Ch., *Introduction to Solid State Physics*, New York: Wiley, 1969.
- [13] Landau, L.D. and Lifshits, E.M., *Kvantovaya Mekhanika: Nerelyativistskaya Teoriya* (Quantum Mechanics: Nonrelativistic Theory), Moscow: Nauka, 1974 (in Russian).
- [14] Landau, L.D. and Lifshits, E.M., *Elektrodinamika Sploshnykh Sred* (Electrodynamics of Continuous Media), Moscow: Nauka, 1982 (in Russian).
- [15] Herring, C. and Flicker, M., Asymptotic Exchange Coupling of Two Hydrogen Atoms, 1964, vol.134, no.2A, pp.A362–A366.
- [16] Berman, G.P., Cambell, D.K., Doolen, G.D. and Nagaev, K.E., Dynamics of the Measurement of Nuclear Spins in a Solid-State Quantum Computer, 1999, E-print LANL: cond-mat/9905200.
- [17] Kane, B.E., McAlpine, N.S., Dzurak, A.S., Clark, R.G., Milburn, G.J., Sun, H.B., and Wiseman, H., Single Spin Measurement Using Single Electron Transistors to Probe Two Electron Systems, 1999, E-print LANL: quant-ph/9903371.

- [18] Waugh, J.S. and Slichter, C.P., Mechanism of Nuclear Spin–Lattice Relaxation in Insulator at Very Low Temperatures, *Phys. Rev. B: Condens. Matter*, 1988, vol. 37, pp. 4337–4339.
- [19] Molotkov, S.N. and Nasin, S.S., Single Spin Detection for the Kane Model of Silicon-Based Quantum Computer, 1999, E-print LANL: quant-ph/9906106.
- [20] Viola, L., Knill, E. and Lloyd, S., Dynamical Decoupling of Open Quantum Systems, 1998, E-print LANL: quant-ph/9809071.
- [21] Turov, E. and Petrov, M.P., Nuclear magnetic resonance in ferromagnetics and antiferromagnetics, Moscow, Nauka, 1969 (in Russian).
- [22] Wei, H., Xue, X. and Morgera, S.D., NMR Quantum Automata in Doped Crystals, 1998, E-print LANL: quant-ph/9805059.
- [23] Gammon, D., Brown, S.W., Snow, E.S., Kennedy, T.A., Katzer, D.S., and Park, D., Nuclear Spectroscopy in Single Quantum Dots: Nanoscopic Raman Scattering and Nuclear Magnetic Resonance, *Science*, 1997, vol. 277, no. 5322, pp. 85–88.
- [24] Luo, J. and Zeng, X., NMR Quantum Computation with a Hyperpolarized Nuclear Spin Bulk, 1998, E-print LANL: quant-ph/9811044.

# Figures

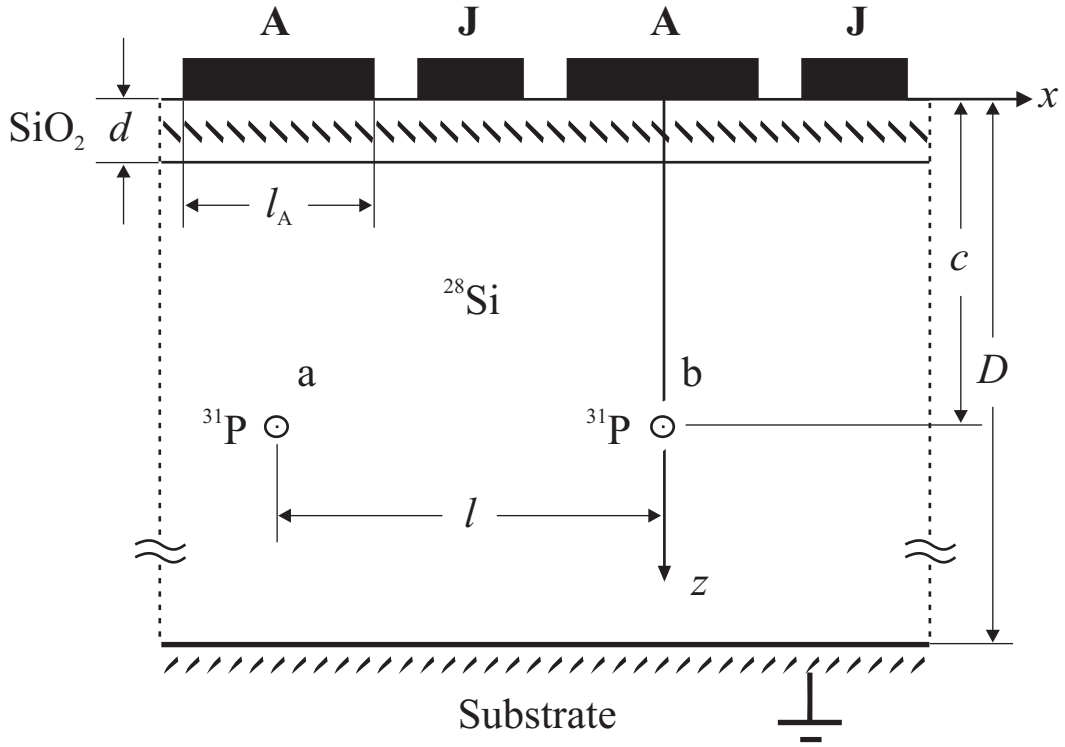


Fig. 1. Two cells of the semiconducting structure with donor atoms a and b.  $l_A \sim 10$  nm,  $l \sim 20$  nm, and  $c \sim 20$  nm [6]

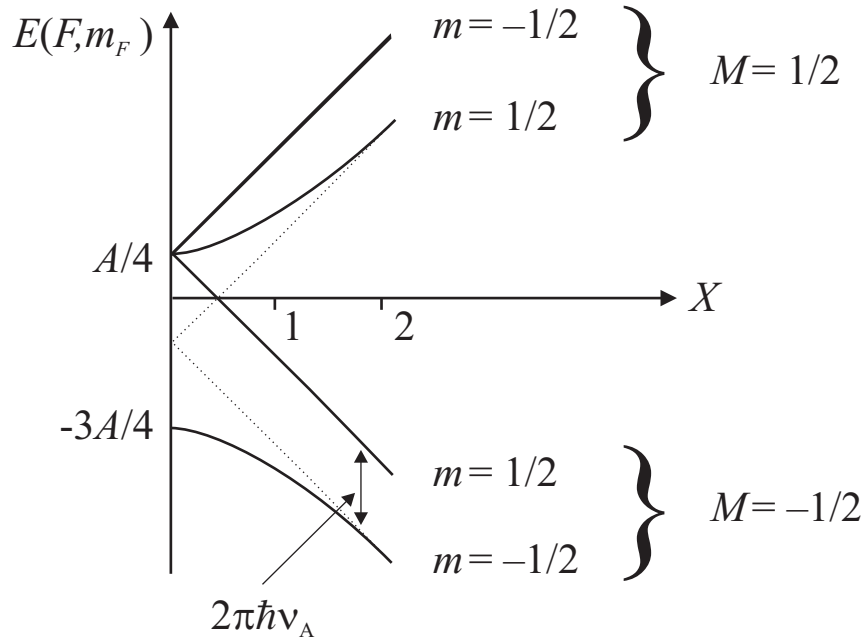


Fig. 2. Energy levels in the electronic–nuclear system of an individual donor atom.

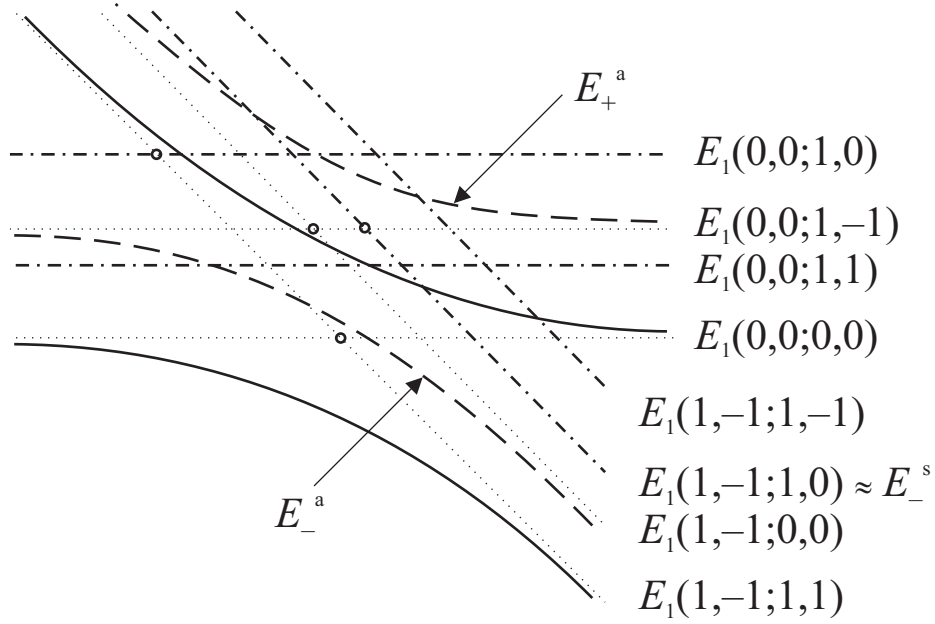
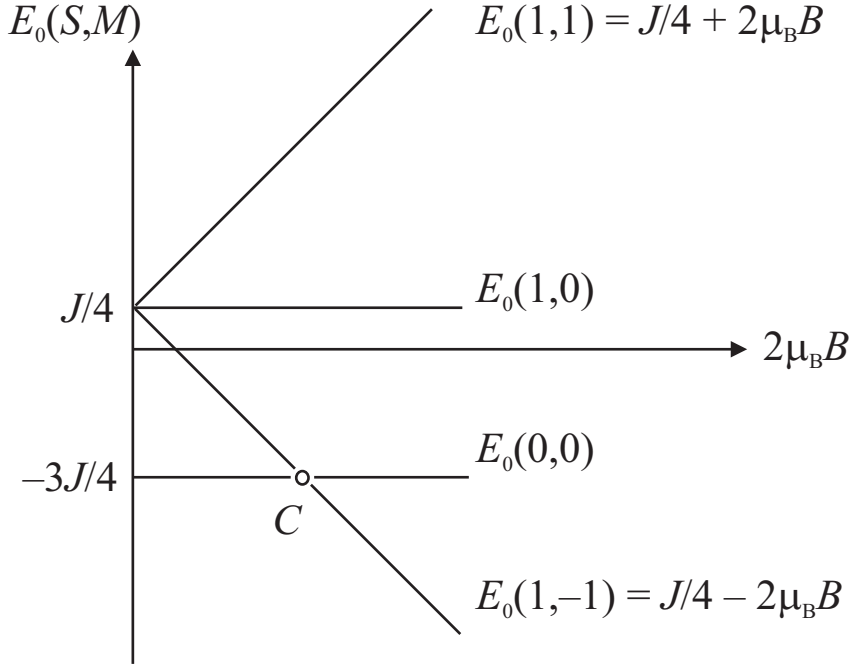


Fig. 3. Energy levels of a dual-spin system subjected to a magnetic field in the absence of nuclear spins. The inset schematically shows hyperfine splitting of the ground electronic states near the crossing point  $C$  for  $A_a \neq A_b$ . The circles indicate the anticrossing points of hyperfine states.

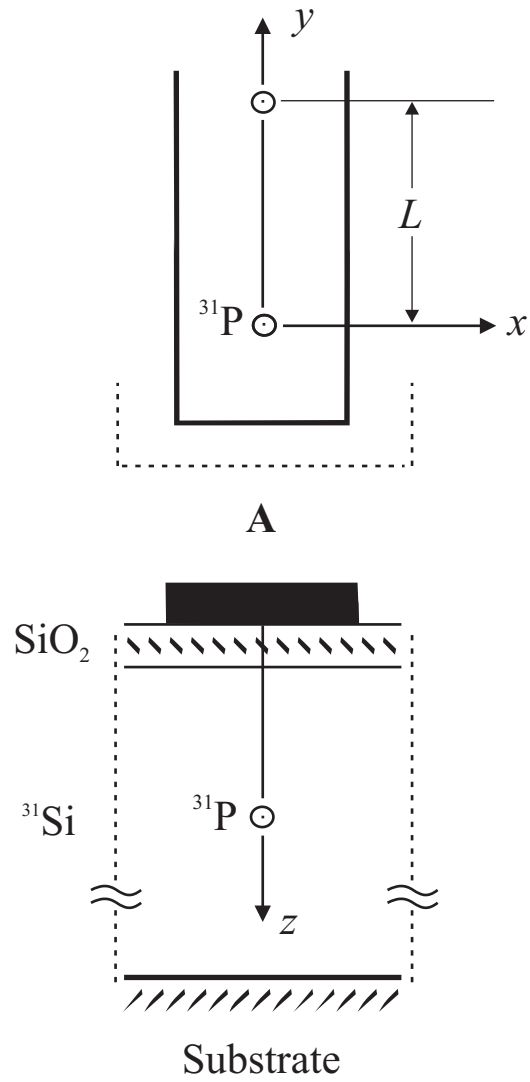


Fig. 4. Fragment of the suggested ensemble structure (region only under gate **A**).